Journal of Environmental Chemical Engineering 5 (2017) 4656–4662

Contents lists available at ScienceDirect

Journal of Environmental Chemical Engineering

journal homepage: www.elsevier.com/locate/jece

High sorption of phosphate on Mg-Al layered double hydroxides: Kinetics and equilibrium

Carina V. Luengo[a,*], María A. Volpe[b], Marcelo J. Avena[a]

[a] INQUISUR, Departamento de Química, Universidad Nacional del Sur (UNS)-CONICET, Bahía Blanca, Argentina
[b] PLAPIQUI, UNS-CONICET, Bahía Blanca, Argentina

ARTICLE INFO

Keywords:
Adsorption
Kinetics
Phosphorus
LDH

ABSTRACT

The development of new materials for environmental remediation is a topic of high priority due to the increasing contamination of water. Although phosphate is not toxic, it has been recognized as one the main species responsible for eutrophication of fresh water bodies, and thus remediation techniques are continuously investigated to remove it from aqueous media. A Mg-Al layered double hydroxide (Mg-Al LDH) was synthesized by the co-precipitation method at constant pH 9. It was characterized by XRD, FTIR, TG-DSC, SEM and TEM, together with dissolution kinetics, phosphate adsorption kinetics, adsorption isotherms and electrophoretic mobilities. The solid was stable at pH > 5 in NaCl aqueous solutions. Lower pH resulted in a fast dissolution, and at pH 3 dissolution was complete after 100 min. Phosphate adsorption kinetics, isotherms and electrophoretic mobility enabled to establish that phosphate adsorbs via three different adsorption modes: anion exchange, electrostatic attraction and surface complexation. The phosphate adsorption capacity of the LDH at pH 5 was 2.25 mmol g^{-1}. This is the highest adsorption value when compared with the performance of other phosphate sorbents in the literature. The synthesized LDH, therefore, is a promising environmentally friendly solid to be used in wastewater treatment systems or to remove phosphate from aquatic environments.

1. Introduction

Phosphorus is an essential macronutrient for all life forms; it is a limiting factor for biological productivity in many terrestrial and marine environments [1]. Phosphorus is often present in wastewater in low concentrations mostly as phosphates, including organic phosphate, inorganic phosphate, oligophosphates and polyphosphates (particulate P). Although it is an essential nutrient, concentrations exceeding the desired limits promote eutrophication of surface waters [2], leading to algae overgrowth, oxygen depletion and fish death. Therefore, there is currently an urgent demand for phosphorus/phosphate removal from aquatic environments [3,4].

Phosphate is released to aquatic environments through weathering of rocks and by various human activities such as industrial, agricultural and household uses [5]. A typical raw domestic wastewater has a total phosphorus concentration of approximately 10 mg/L with orthophosphate as the main form of phosphate. The World Health Organization (WHO) has set a maximum discharge limit of phosphorus of 0.5–1 mg/L as a guideline [6]. Thus, treatment prior to discharge into natural streams is inevitable in order to meet the standard of water quality.

Although various physical methods such as crystallization, electrodialysis and reverse osmosis are available, removal of phosphate from polluted and wastewaters is mainly carried out either by chemical precipitation or adsorption. Chemical precipitation is an effective method for high concentration phosphate removal, but it requires sophisticated control systems. The adsorption method proves to be more effective due to its low cost, higher uptake capacity, greater selectivity, faster regeneration kinetics, less production of sludge and easy operation [3].

Numerous materials have been used by different researchers as adsorbents for phosphate removal, such as waste materials (red mud, fly ash), zeolite and titanium dioxide, activated alumina, calcite, goethite, zirconium hydroxide and activated carbon [7]. In addition, there is a growing interest in the use of layered double hydroxides (LDHs) as phosphate adsorbents. LDHs are promising materials because they may have a very high sorption capacity [8].

LDH, also known as hydrotalcite-like-compounds or anionic clays, have been widely used as adsorbents [9–14]. The general formula of LDHs is $[M^{2+}_{1-x}M^{3+}_{X}(OH)_2]^{x+}[A^{n-}]_{x/n}\cdot yH_2O$, where M^{2+} and M^{3+} are divalent and trivalent metal cations, respectively, A^{n-} is an anion incorporated in the interlayer space along with water molecules for charge neutrality and structure stability. The identities of M^{2+}, M^{3+}

* Corresponding author.
E-mail address: cluengo@uns.edu.ar (C.V. Luengo).

http://dx.doi.org/10.1016/j.jece.2017.08.051
Received 19 April 2017; Received in revised form 23 August 2017; Accepted 25 August 2017
Available online 01 September 2017

and A^{n-}, and the value of x may vary over a wide range, thus giving rise to a large class of isostructural materials with varied physicochemical properties [15].

LDHs are layered materials with hydroxide sheets, where a net positive charge is developed on the layer due to partial isomorphic substitution of trivalent for divalent cations, balanced by exchangeable anions and water molecules, which are intercalated in the interlayer space between two brucite sheets. The interlayer anions can be exchanged for other anions with higher selectivity [8].

Due to the high charge density of the sheets, large interlayer areas (around 1000 $m^2\ g^{-1}$), good thermal stability, flexible interlayer region accommodating various anionic species and high anion exchange capacities of the interlayer anions (3.0–4.8 meq g^{-1}), LDHs have been employed in several studies for removing different anionic species from aqueous systems, such as fluoride, selenite, arsenate, perchlorate, chromate, phosphate, vanadate, antimonite [15–22].

In the present work, a Mg-Al-LDH was studied as an adsorbent for phosphate removal from aqueous solution. This solid was selected because it is not harmful for the environment [23]. The effects of various experimental conditions such as contact time, pH, and phosphate concentration were investigated. The adsorption mode of phosphate onto LDH is discussed, and its performance is analyzed by comparing the adsorption capacity of many other phosphate sorbents.

2. Materials and methods

2.1. Sample synthesis

All solutions were prepared with double distilled deionized water, boiled and purged with N_2, and reagent grade chemicals. The synthesis was done at room temperature and under a stream of N_2 in order to minimize contamination by atmospheric CO_2.

Mg-Al-LDHs were prepared by the coprecipitation method at constant pH [15]. A 100 mL mixture of $MgCl_2$ and $AlCl_3$ aqueous solution, with $[Mg^{2+}]/[Al^{3+}] = R = 2$ ratio and $[Mg^{2+}] + [Al^{3+}] = 1$ M was added dropwise into a flask containing 100 mL of a 1 M NaCl solution. The addition was performed under vigorous stirring at pH = 9, fixed with a 2 M NaOH solution. The synthesis was performed under nitrogen bubbling in order to minimize carbonate intercalation. Once the reactants addition finished, the mixture was maintained under stirring, nitrogen bubbling and pH control for 2 h. The obtained solid was then separated by centrifugation, washed several times with water and finally dried in air at 60 °C. Then, the solid was gently grinded using mortar and pestle.

2.2. Structural characterization of the solid before and after phosphate adsorption

Mg content was determined by atomic absorption spectrometry in a GBC Avanta 932 instrument. Al content was measured by ICP in a Shimadzu Simultaneous 9000 device. Prior quantifications, the solid was dissolved in concentrated HCl (37%) and afterwards diluted with water to fit the calibration range. C, H and N quantification was performed in an Exeter Analytical INC model CE440 autoanalyzer.

The content of surface and interlayer water was determined by thermogravimetric analysis (TG) from the weight loss below 210 °C using a 5 °C min^{-1} heating rate. This analysis, together with Differential Scanning Calorimetry (DSC) were performed with a STD Q600 TA instrument.

SEM and TEM images were obtained with an EVO 40-XVP and a JEOL- 100 CX II microscopes, respectively. Powder X ray diffraction (PXRD) patterns were recorded in a Rigaku Geigerflex diffractometer between 2° and 60° 2θ using Cu Kα radiation. FT-IR spectra were obtained from KBr pellets (1% weight sample in KBr) in a Nicolet Magna 560 FTIR instrument equipped with DTGS detector. A nitrogen adsorption isotherm (BET) was performed in order to quantify surface area at 77 K using a Micromeritics ASAP 2000 instrument.

2.3. Dissolution kinetics

The dissolution of the solid particles at constant pH was studied by dispersing 0.03 g of LDH in 100 mL of 0.1 M NaCl [24,25]. The pH of the dispersion was adjusted to the desired value and it was kept constant during all the experiment by adding minute volumes of concentrated NaOH or HCl solutions. The suspension was continuously mixed with a magnetic stirrer. At different reaction times, a 10 mL aliquot was withdrawn, immediately centrifuged at 5000 rpm during 10 min and the supernatant extracted for Mg analysis. The reaction was followed for 400 min. Since centrifugation lasted 10 min, a ± 5 min error bar covers all the time needed for centrifugation. This error bar is usually the size of the symbol used to represent each data point. The studies were made in the pH range 3.0-8.0 in order to evaluate the effect of pH on the stability of the solid. The reaction temperature was 25 ± 0.2 °C.

2.4. Batch adsorption kinetics

A batch technique was used to investigate the kinetics of phosphate adsorption [26,27]. The reaction was carried out in a cylindrical, water-jacketed reaction vessel covered with a glass cap. Mixing was performed by a magnetic stirrer, and carbon dioxide contamination was avoided by bubbling water-saturated N_2. The reaction temperature was maintained at 25 ± 0.2 °C by circulating water through the jacket with a FAC (Argentina) water bath/circulator.

A series of experiments was performed at constant pH 5.0 and varying initial phosphate concentrations to investigate the effect of phosphate concentration. Other experiments were performed at constant initial phosphate concentration and varying pH in order to investigate pH effects. In the first case, 100 mL of a 0.1 M NaCl solution were placed in the reaction vessel, and the stirring, N_2 bubbling and water circulation were switched on. Once the temperature reached the desired value, the pH of the NaCl solution was adjusted to pH 5.0. Then, 0.03 g of LDH was added to the vessel and the dispersion was stirred for 15 min. The kinetic experiment was started by adding a known volume of either a 1.6×10^{-3} M or a 1.6×10^{-1} M phosphate solution to attain initial concentrations between 5.6×10^{-5} M and 3.2×10^{-3} M. At different reaction times, a 5 mL aliquot was withdrawn, immediately centrifuged at 5000 rpm during 10 min and the supernatant extracted for phosphate analysis. The reaction was followed for 500 min and the pH was continuously checked and kept constant by adding minute volumes (microliters) of concentrated NaOH or HCl solutions. The same procedure was employed to investigate the effects of pH (5.0, 7.0 and 9.0) at an initial phosphate concentration of 1.6×10^{-3} M. Comparative experiments showed that separating the supernatant from the solid phase using 10 min centrifugation renders the same results as filtering the dispersion with cellulose acetate filters (Supplementary material).

Phosphate concentrations were measured by the method proposed by Murphy and Riley [28], which use an acidified solution of ammonium molybdate containing ascorbic acid and a small amount of antimony. The phosphate complex concentration was measured at 880 nm using an Agilent 8453 UV–vis diode array spectrophotometer equipped with a quartz cell of a 1-cm optical pathlength. Calibration curves were obtained with phosphate concentrations ranging from 5.0×10^{-6} M to 3.2×10^{-5} M. According to Gao and Mucci [29], the detection limit of this technique is around 0.01 μM. The error in the slope, using 19 calibration curves, was 1.7%. Adsorbed phosphate was calculated from the difference between the initial oxyanion concentration and the concentration that remained in the supernatant solution.

In all experiments, the pH was measured with a Crison GLP 22 pH meter and a Radiometer GH2401 combined pH electrode. The stirring of the dispersions was done with an IKA RH digital KT/C stirrer with

stirring rate control, which ensures good mixing and allows keeping a constant solid-to-solution ratio during the experiment [24].

2.5. Electrophoretic mobility

A Malvern Zetasizer Nano ZS90 electrophoresis apparatus was used to measure the electrophoretic mobility of LDH particles before and after phosphate adsorption. For the bare solid, 0.05 g of the material were added to 50 mL of a 0.01 M NaCl solution and dispersed by stirring for 15 min. The pH of this dispersion was decreased to approximately 4.5 with an HCl solution and afterwards increased adding NaOH until pH = 11.5 in 0.5-1 pH-units steps. In each step the suspension was stirred for 5 min and the pH and electrophoretic mobility (μ) was measured [15]. Electrophoretic mobilities were converted to zeta potentials (ζ) with the Smoluchowski equation [30],

$$\upsilon_E = \frac{\varepsilon\zeta}{\eta}$$

where ε is the dielectric constant, ζ is the zeta potential and η is the viscosity. Similar experiments were done for the solid in the presence of different phosphate concentrations (between 3.16×10^{-5} M and 8×10^{-4} M). 0.05 g of the solid were added to 50 mL of a 0.01 M NaCl solution and dispersed by stirring for 15 min. Then, a known concentration of phosphate was added, allowing the system to equilibrate for ten minutes. The pH of this dispersion was decreased to approximately 4.5 and afterwards increased step-by-step until pH = 11.5, measuring the mobility as indicated above.

3. Results and discussion

3.1. LDH characterizations

Chemical analysis gave 23.98% for Mg, 15.25% for Al, 1.25% for C and 13.9% for H_2O leading to the chemical formula $[Mg_{0.64}Al_{0.36}(OH)_2]Cl_{0.34}(CO_3)_{0.01}.0.50H_2O$. The small content of CO_3^{2-} is likely originated from atmospheric CO_2. According to the chemical formula, the studied solid has a structural positive charge of 4.44 meq g^{-1}. This value was calculated taking into account that for each Mg atom that is replaced by an aluminum atom, a positive charge is generated within the LDH structure. According to the chemical formula, the LDH has a positive charge of 0.36 eq (which is neutralized by 0.34 eq of chloride plus 0.02 eq of carbonate). Taking into account the chemical formula weight, the resulting structural charge is 4.44 meq g^{-1}.

The TG curve of Mg-Al LDH is shown in Fig. 1. It displays two overlapped endothermic weight losses between 25 and 260 °C (peaks at 121 °C and 195 °C) summing 16.4% corresponding to the loss of surface and intercalated water [31], and other two overlapped endothermic weight losses between 260 and 700 °C (peaks at 356 °C and 397 °C) summing 27.9% due to the loss of OH groups. There was also a small weight loss of 3.0% between 700 and 1100 °C.

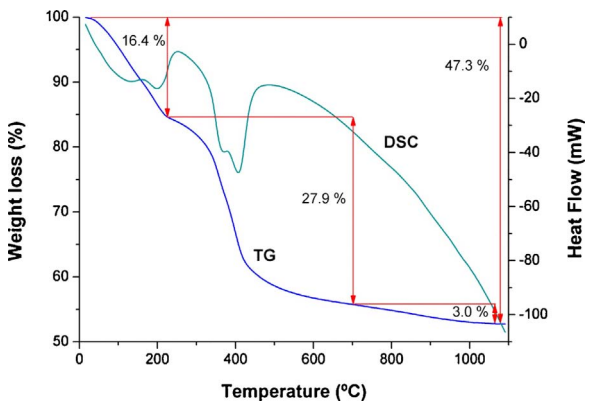

Fig. 1. TG with DSC of Mg-Al LDH.

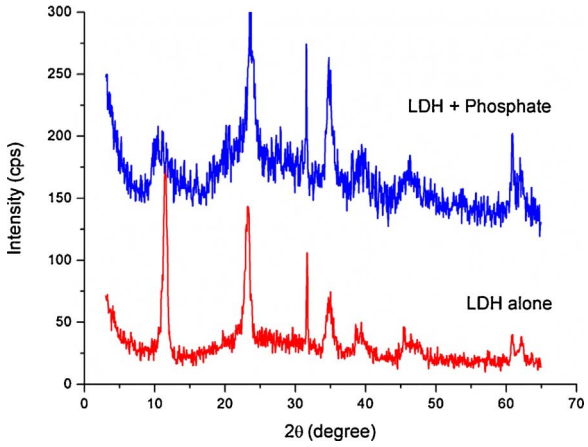

Fig. 2. XRD patterns of Mg-Al LDH before and after phosphate adsorption. Used phosphate concentration was 1.6×10^{-3} M, corresponding to an adsorbed amount (P_{ads}) of 1.25 mmol g^{-1}.

The SEM and TEM micrographs of Mg-Al LDH are shown as Supplementary material. A layered structure was observed, with overlapping plate-like particles having a size of 50–100 nm. This structure is typical of LDH materials [1,17,32,33].

The XRD patterns of Mg-Al LDH before and after phosphate adsorption are shown in Fig. 2. Although somewhat noisy, probably because of random orientation of particles, LDH before phosphate adsorption shows the typical XRD pattern of a pure hydrotalcite. The peaks at 2θ = 11.68° (7.57 Å) and 23.24° (3.78 Å), corresponding respectively to (003) and (006) diffraction planes, are characteristic of these layered structures [34]. The basal spacing d_{003} = 7.57 Å results from the sum of the brucite-type layer (4.80 Å) of the solid and the interlayer space (2.77 Å) with the intercalated anions (mainly Cl^-). The lattice parameters $a = 2d_{110}$ = 3.04 Å, which is the cation–cation distance in the brucite-like layer, and $c = 3d_{003}$ = 22.71 Å, which is related to the thickness of the brucite-like layers and the interlayer space, were those expected for a Mg-Al hydrotalcite sample with Mg-Al = 2 and most of the charge-balancing anions being Cl^- [34].

Phosphate adsorption produced loss of crystallinity of the solid and an enlargement of the basal spacing d_{003} to 8.43 Å, indicating the expansion of the interlayer because of phosphate intercalation. Since the thickness of brucite-like layers is 4.77 Å [35], the interlayer space can be calculated as 2.80 Å in absence of phosphate and 3.66 Å with adsorbed phosphate. Similar changes were reported by other authors [1,34,36,37].

The measured N_2 adsorption area was 26 m^2 g^{-1}. N_2 adsorption is not commonly used to measure the specific surface area of layered materials like LDH because N_2 cannot enter the interlayer space, and therefore only the external area of the sample is quantified. The total specific surface area (including the area of the interlayer space) can be theoretical calculated from XRD data and chemical formulae ($S = 3^{½}a^2N/M$), where a is the unit cell parameter, N is the Avogadrós constant, and M is the chemical formula weight) [16]. This area was found to be 1214 m^2 g^{-1}. Since phosphate enters the interlayer space, it senses the total area of the solid.

Fig. 3 presents the FTIR spectra of the solid before and after phosphate adsorption. They are also typical hydrotalcite-like materials. The spectrum in absence of phosphate shows a broad band at around 3447 cm^{-1} (O–H stretching vibration in the brucite-like sheets and water in the interlayer space), a band at 1636 cm^{-1} (water bending vibration of interlayer water), and bands at 790, 669 and 552 cm^{-1} (M–O stretching and M–O–H bending, M = Mg, Al) [4,38]. The band at 1356 cm^{-1} shows the existence of CO_3^{2-} species in the interlayer [3,39,40].

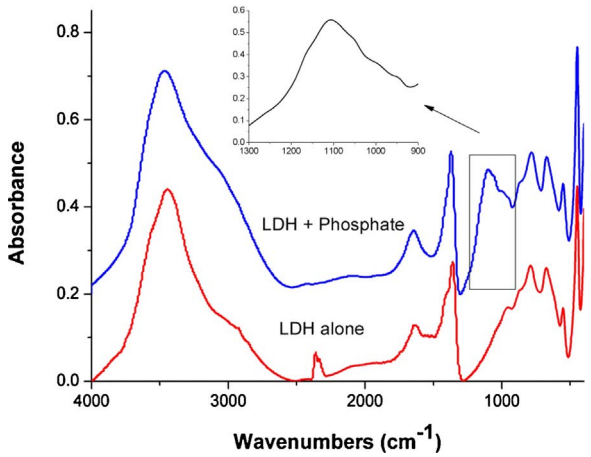

Fig. 3. FTIR spectra of Mg-Al LDH before and after phosphate adsorption. Used phosphate concentration was 1.6×10^{-3} M, corresponding to an adsorbed amount (P_{ads}) of 1.25 mmol g^{-1}.

After adsorption of phosphate the characteristic P-O stretching vibration appears at 1098 cm^{-1} [3,4,11,40], confirming that phosphate was successfully adsorbed on LDH.

3.2. Dissolution kinetics

Dissolution kinetic results are shown in Fig. 4. The dotted line indicates complete dissolution as calculated from the Mg content of the sample. The kinetics was very similar in the pH range 5–8, where only a fraction of the solid was dissolved (around 22%). The dissolution was higher and faster in the pH range 3–4, being almost complete at pH 3 after 150–200 min of reaction.

It emerges from the data that the studied LDH must be used in the pH range 5–8 in order to impede very high dissolution. Even in this pH range, a 22% dissolution is not negligible at all, and is quite normal for LDHs [25]. This is why a Mg-Al LDH was selected, since the solid or its dissolution products, Al(III) and Mg(II) aqueous species, are not toxic for the environment [23].

3.3. Phosphate adsorption kinetics

Fig. 5 shows the phosphate adsorption kinetics at pH 5.0. The different curves adsorbed phosphate (P_{ads}) vs. time (t) were obtained with different initial phosphate concentrations. pH 5.0 was chosen for the adsorption kinetics study because was observed that it was the pH

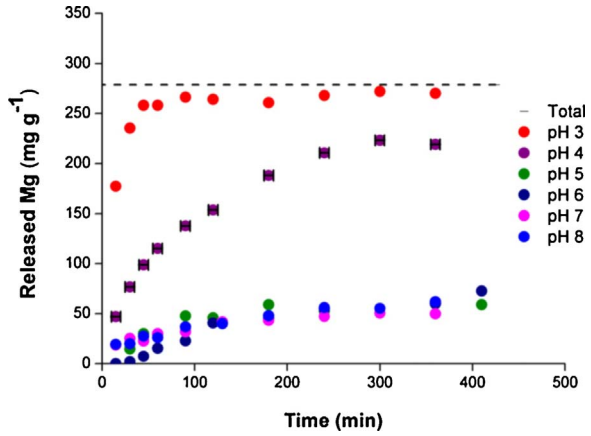

Fig. 4. Dissolution kinetics of Mg-Al LDH at different pH. Dotted line indicates the theoretical complete dissolution. Time error bars (± 5 min) are shown as an example in data of pH 4, and cover the time lasted from the beginning until the end of centrifugation.

where the highest adsorption of phosphate was produced. All curves have similar characteristics, showing a fast initial adsorption and a slower adsorption at longer times. Error bars suggest that equilibrium or near equilibrium conditions were attained at about 300 min. The results are in agreement with those reported in several other articles where oxyanion adsorption was studied [17,18,41].

The effects of pH on phosphate adsorption kinetics are depicted in Fig. 6, which shows data obtained at constant initial phosphate concentration (1.6×10^{-3} M) and varying pH (5.0, 7.0 and 9.0).

The adsorption was rather fast during the first 20 min at all investigated pH values. After that, the adsorption became slow at pH 9.0, and increased as pH decreased. Some authors interpreted the effects of pH on the adsorption rate as a consequence of the competition between OH^- groups and phosphate species for adsorption sites [2,4,11,16]. Indeed, at constant phosphate concentration the competition will increase if pH is increased. Some other authors, on the contrary, attributed this kinetic behavior to an electrostatic effect [5,11,16]. At phosphate concentrations higher than 8×10^{-4} M and pH > 5, which is the case of our experiments, LDH particles acquired a net negative charge that increased as pH increased (see zeta potential data below). This increase in the negative charge would increase the electrostatic repulsion between LDH and adsorbing phosphate, decreasing the adsorption rate. A third group of authors, on the contrary, attributed the changes in the adsorption rate with pH to changes in LDH solubility [1]. As pH decreases, the solubility increases, and Mg^{2+} and Al^{3+} cations are released to the solution, capturing phosphate ions and thereby increasing phosphate removal [42].

The evidence so far does not allow us to select conclusively one of the three processes. The third one can be in principle discarded because it should be only operative at pH < 5, where solubility increases significantly (Fig. 4). Therefore, the behavior seen in Fig. 6 seems to be controlled by a combination of phosphate/hydroxyl competition and electrostatic interactions.

3.4. Adsorption isotherm

From kinetic data at different phosphate concentrations and pH 5.0, and at long adsorption times in Fig. 5, the experimental adsorption isotherm was constructed, and it is shown in Fig. 7.

The adsorption capacity of phosphate onto Mg-Al LDH was around 2.25 mmol g^{-1} at pH 5.0 at the highest investigated equilibrium concentration, C_{eq}, of 2.5×10^{-3} mmol L^{-1}. This adsorption value is only slightly lower than the maximum adsorption capacity that could be calculated using the Langmuir equation (2.40 mmol g^{-1}), suggesting that the solid is near saturation. If adsorption takes place mainly by anion exchange with interlayer chloride ions, and taking into account that the structural charge of the studied solid is 4.44 meq g^{-1}, the observed maximum adsorption is very close to the theoretical adsorption capacity of the synthesized material assuming that phosphate is mainly present in the interlayer as the monoprotonated HPO_4^{2-} species. However, according to the pKa values of phosphoric acid, in the aqueous solution at pH 5.0 the prevailing (almost 100%) species is the biprotonated one, $H_2PO_4^-$. If the adsorbed species is this last one, the observed adsorption only exchanged around 50% of the chloride ions.

3.5. Electrophoretic mobility

Zeta potential vs. pH data (obtained with electrophoretic mobility measurements) of LDH Mg-Al at different NaCl concentrations and in absence of phosphate are shown in Supplementary material. LDH showed positive ζ at all studied pH and ionic strengths. Within experimental error, curves ran rather flat up to pH around 10 and then ζ decreased as pH increased. This ζ vs pH behaviour is rather typical for LDHs, with the positive structural charge controlling most of the electrokinetic properties of the solid. The decrease in ζ at pH > 10 is due to deprotonation of hydroxyl groups, although this deprotonation was

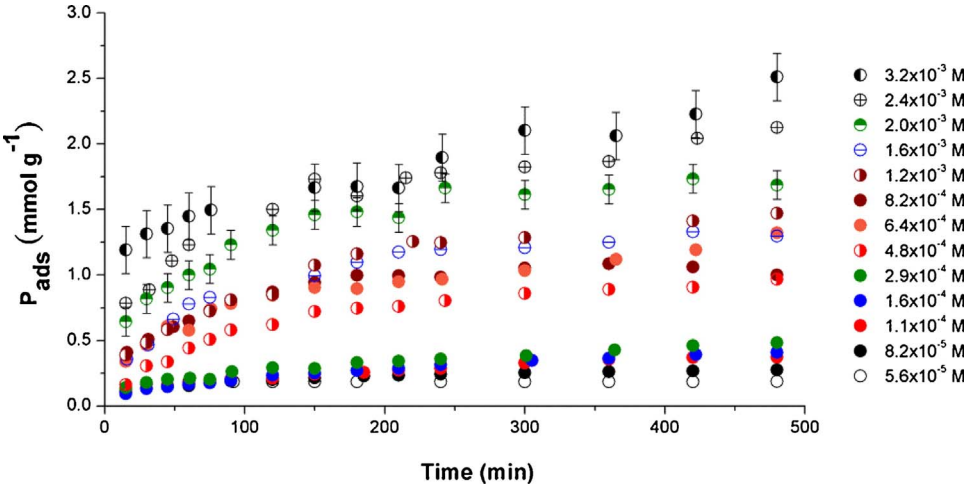

Fig. 5. Adsorption kinetics of phosphate onto Mg-Al LDH at different initial concentrations of phosphate (pH 5.0, 25 °C). Error bars are shown as examples in data of 3.2×10^{-3} M and 2.0×10^{-3} M, and were estimated from the error in phosphate quantification.

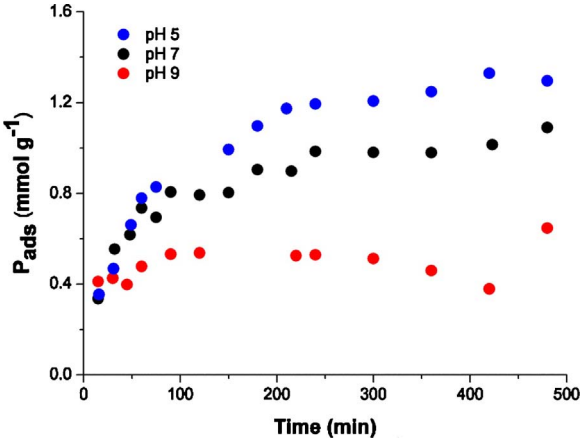

Fig. 6. Adsorption kinetics of phosphate onto Mg-Al LDH at different pH (25 °C, 1.6×10^{-3} M).

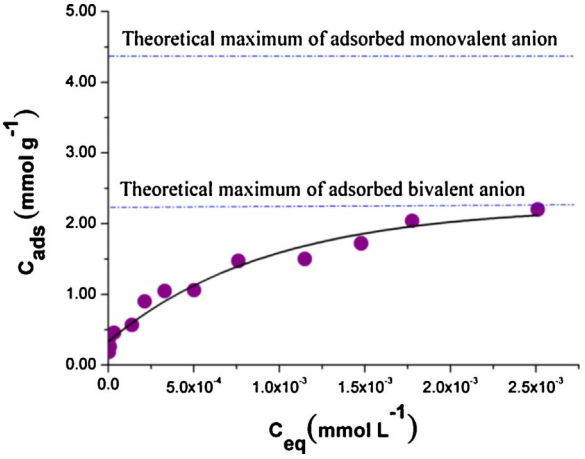

Fig. 7. Phosphate adsorption isotherm on Mg-Al LDH at pH 5.0.

not enough to overcome the structural charge effects. The trend of the curves suggests that the isoelectric point (IEP) of the bare LDH would be close to 13, which agrees with values reported by other authors [1,43,44].

Fig. 8 shows zeta potential vs pH data at different initial phosphate concentration.

As indicated above, in absence of phosphate ζ was positive in the investigated pH range, as a consequence of the net positive charge of

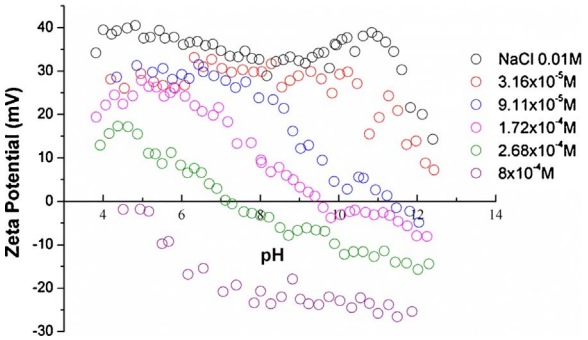

Fig. 8. Zeta potential of Mg-Al LDH at varying phosphate concentrations.

the particles. This charge creates a favorable chemistry for binding negatively charged phosphate species. At a given pH, ζ decreased as phosphate concentration increased. At low phosphate concentrations ζ remained positive at all pH values. However, at higher concentrations the particle showed distinct IEP values, which decreased as phosphate concentration increased. Already at concentration 8×10^{-4} M the particles showed negative ζ in all the pH range studied.

Electrokinetic results usually give valuable information to get a better understanding on how phosphate adsorbs on LDH. There are three possible adsorption modes of phosphate species on the studied solid, which are schematized in Fig. 9. 1) anion exchange, 2) electrostatic attraction, and 3) surface complexation. Anion exchange involves exchange between the entering anions (phosphate species) and the leaving anions (chloride ions). Two possible exchange reactions were mentioned, with either HPO_4^{2-}, or $H_2PO_4^-$ species entering the interlayer space and Cl^- leaving it. Actually, a pure anion exchange process implies no change in the net charge of the particles, thus no change in ζ should be observed in the presence of phosphate. The second adsorption mode is driven by electrostatics. In this case, the positive structural charge of the solid or positive charges generated by protonation of hydroxyl groups at the edges attract negatively charged phosphate species, which remain adsorbed because of coulombic forces. If pure electrostatic interaction takes place, phosphate will adsorb until the positive charge of the solid is completely neutralized, with no extra adsorption after this charge neutralization. This means that in the hypothetical case of pure coulombic interactions no reversal in the sign of ζ should be observed, which is not the case of Fig. 8. The third adsorption mode is surface complexation. This is a common adsorption mode for phosphate species in aluminum, iron and other metal oxides and hydroxides. In surface complexation the adsorbing species acts as a ligand that binds directly metal ions at the surface. In this case, phosphate species act as the entering ligands and hydroxyl ions, which were

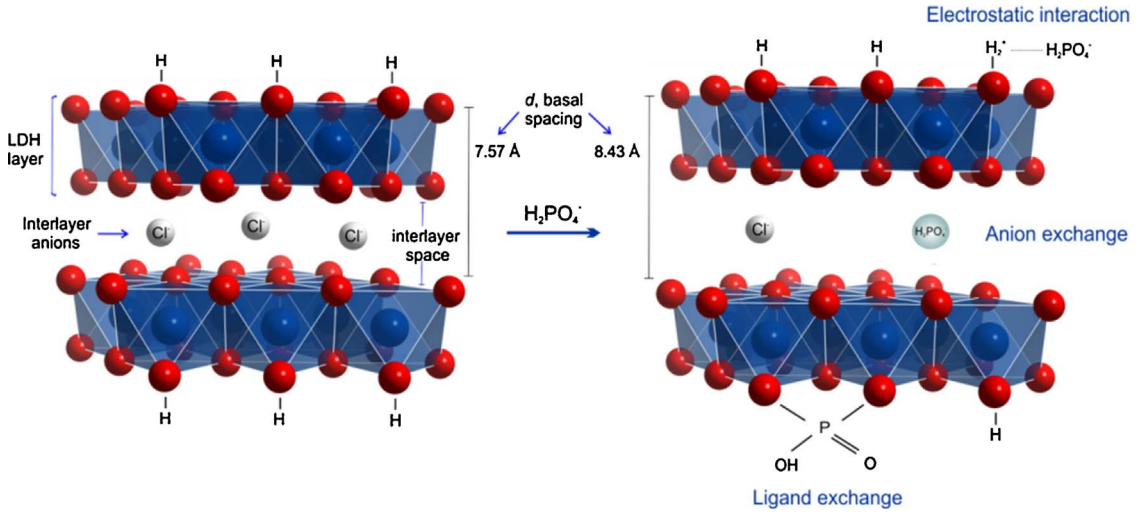

Fig. 9. Schematic drawing showing the three possible adsorption modes of phosphate species on LDH.

Table 1
Phosphate adsorption capacity of different adsorbents.

Adsorbents	Max. adsorption capacity (mmol g^{-1})	pH	Ref.
Fe-Al hydroxides	1.67	4.5	[52]
AlOOH	1.08	4.0	[53]
β-FeOOH	0.55	5.0	[54]
Fe-Mn binary oxide	1.16	5.6	[55]
Mesoporous ZrO_2	0.96	6.8	[56]
MCM-48	1.09	5.0	[57]
Fe-Al-Mn oxide	1.56	6.8	[58]
MnO_2	0.01	6.8	[59]
La_2O_3-zeolite	0.79	6.0	[60]
Mg-Fe-CO_3 LDH	0.45	8.4	[42]
Calcined Mg-Mn LDH	1.10	8.0	[61]
Calcined Mg-Al LDH	1.42	6.0	[2]
Uncalcined Mg-Al LDH	2.07	6.0	[63]
Mg-Al LDH	2.25	5.0	This study

bonded to Al(III) or Mg(II) ions at the surface, act as the leaving ligands. Surface complexation of phosphate is rather strong and normally overcomes electrostatic repulsion. This means that charge reversal from positive to negative can easily takes place, which is the observed case. This result is also showed by Morimoto et al. [44]. In summary, electrokinetic results indicate that neither anion exchange nor electrostatic attraction can be the only operating mode for adsorption. Some ligand exchange must exist in order to explain the changes in ζ.

The analysis of electrokinetics in conjuction with other results suggests that the three adsorption modes are likely to operate in the studied system. XRD data showed that phosphate species enter the interlayer space of LDH, giving good evidences for anion exchange. Electrokinetics support the adsorption via ligand exchange. There is no result that allows experimentally confirm or reject electrostatic interaction, but it is clear that they are always present in ion adsorption on charged surfaces.

3.6. Comparing the phosphate adsorption capacity of different solids

Many papers have been published in the literature where the central aim was to evaluate the ability of different materials as phosphate adsorbents. For example, the adsorption capacity of waste materials or by-products such as red mud [45], fly ash [46], blast furnace slag, calcined alunite [47], activated alumina [48], activated coir pith carbon [49] and manganese nodules leached residue [50], metal oxide hydroxides [51–54], metal oxides [55–60], and LDHs [42,61–63] and their calcined products [2,61,64], were tested. Table 1 summarizes the adsorption capacities of the mentioned materials, including the LDH studied in this work.

The Mg-Al LDH synthetized in this study exhibits significantly higher adsorption capacity for phosphate than the other materials. The studied solid even shows a better performance than other Mg-Al LDH. This ability, combined with the facts that the material is not harmful for the environment, is simple to prepare, and has good thermal stability, make the studied solid promising for phosphate sorption in wastewater treatment systems. It must be noted, however, that there is one disadvantage arising from the high affinity of the solid for phosphate: it cannot be reused in different adsorption cycles. The only way of desorbing attached phosphate is to use a displacing anion with higher affinity for the surface than phosphate, what will in turn impede the reuse of the LDH for adsorbing phosphate. This is the price that is needed to pay in order to have a good phosphate removal.

4. Conclusions

An environmentally friendly LDH was synthetized and tested for phosphate adsorption under different conditions. A combination of adsorption kinetics, adsorption isotherm and electrophoretic mobility enabled to establish that phosphate adsorbs via three different adsorption modes: anion exchange, electrostatic attraction and surface complexation. The adsorption capacity of the studied LDH was very good, better than all other phosphate sorbents published in the literature. The solid results then promising for phosphate uptake in wastewater treatment systems.

Acknowledgments

This work was financed by UNS, ANPCYT and CONICET.

Appendix A. Supplementary data

Supplementary data associated with this article can be found, in the online version, at http://dx.doi.org/10.1016/j.jece.2017.08.051.

References

[1] C. Novillo, D. Guaya, A. Allen-Perkins Avendaño, C. Armijos, J.L. Cortina, I. Cota, Evaluation of phosphate removal capacity of Mg/Al layered double hydroxides from aqueous solutions, Fuel 138 (2014) 72–79.
[2] J. Das, B.S. Patra, N. Baliarsingh, K.M. Parida, Adsorption of phosphate by layered double hydroxides in aqueous solutions, Appl. Clay Sci. 32 (2006) 252–260.
[3] K. Yang, L. Yan, Y. Yang, S. Yu, R. Shan, H. Yu, B. Zhu, B. Du, Adsorptive removal of phosphate by Mg–Al and Zn–Al layered double hydroxides: kinetics, isotherms and

mechanisms, Sep. Purif. Technol. 124 (2014) 36–42.
[4] Y. Yu, J.P. Chen, Key factors for optimum performance in phosphate removal from contaminated water by a Fe–Mg–La tri-metal composite sorbent, J. Colloid Interf. Sci. 445 (2015) 303–311.
[5] R. Chitrakar, S. Tezuka, A. Sonoda, K. Sakane, K. Ooi, T. Hirotsu, Adsorption of phosphate from seawater on calcined MgMn-layered double hydroxides, J.Colloid Interf. Sci. 290 (2005) 45–51.
[6] Department of natural resources. Chapter NR 217. Effluent standards and limitations for phosphorus. https://www.epa.gov/sites/production/files/2014-12/documents/wiwqs-nr217.pdf.
[7] H. He, H. Kang, S. Ma, Y. Bai, X. Yang, High adsorption selectivity of ZnAl layered double hydroxides and the calcined materials toward phosphate, J. Colloid Interf. Sci. 343 (2010) 225–231.
[8] R. Rojas, Layered double hydroxides applications as sorbents for environmental remediation, in: A.C. Carillo, D.A. Griego (Eds.), Hydroxides: Synthesis, Types and Applications, Nova Science Pub Inc., UK, 2012, pp. 39–72.
[9] Y. Wu, Y. Yu, J.Z. Zhou, J. Liu, Y. Chi, Z.P. Xu, G. Qian, Effective removal of pyrophosphate by Ca–Fe–LDH and its mechanism, Chem. Eng. J. 179 (2012) 72–79.
[10] A. Halajnia, S. Oustan, N. Najafi, A.R. Khataee, A. Lakzian, Adsorption–desorption characteristics of nitrate, phosphate and sulfate on Mg–Al layered double hydroxide, Appl. Clay Sci. 80–81 (2013) 305–312.
[11] P. Cai, H. Zheng, C. Wang, H. Ma, J. Hu, Y. Pu, P. Liang, Competitive adsorption characteristics of fluoride and phosphate on calcined Mg–Al–CO_3 layered double hydroxides, J. Hazard. Mater. 213–214 (2012) 100–108.
[12] T. Kameda, H. Takeuchi, T. Yoshioka, Uptake of heavy metal ions from aqueous solution using Mg–Al layered double hydroxides intercalated with citrate, malate, and tartrate, Sep. Purif. Technol. 62 (2008) 330–336.
[13] L. Lv, Defluoridation of drinking water by calcined MgAl-CO_3 layered double hydroxides, Desalination 208 (2007) 125–133.
[14] Z.M. Ni, S.J. Xia, L.G. Wang, F.F. Xing, G.X. Pan, Treatment of methyl orange by calcined layered double hydroxides in aqueous solution: adsorption property and kinetic studies, J. Colloid Interf. Sci. 316 (2007) 284–291.
[15] R. Rojas Delgado, C.P. De Pauli, C. Barriga Carrasco, M.J. Avena, Influence of MII/MIII ratio in surface-charging behavior of Zn–Al layered double hydroxides, Appl. Clay Sci. 40 (2008) 27–37.
[16] R. Rojas, F. Bruna, C.P. de Pauli, M.A. Ulibarri, C.E. Giacomelli, The effect of interlayer anion on the reactivity of Mg–Al layered double hydroxides: improving and extending the customization capacity of anionic clays, J. Colloid Interf. Sci. 359 (2011) 136–141.
[17] K.H. Goh, T.T. Lim, Z. Dong, Application of layered double hydroxides for removal of oxyanions: a review, Water Res. 42 (2008) 1343–1368.
[18] F.L. Theiss, S.J. Couperthwaite, G.A. Ayoko, R.L. Frost, A review of the removal of anions and oxyanions of the halogen elements from aqueous solution by layered double hydroxides, J. Colloid Interf. Sci. 417 (2014) 356–368.
[19] H. Lu, Z. Zhu, H. Zhang, J. Zhu, Y. Qiu, Simultaneous removal of arsenate and antimonate in simulated and practical water samples by adsorption onto Zn/Fe layered double hydroxide, Chem. Eng. J. 276 (2015) 365–375.
[20] N. Chubar, M. Szlachta, Static and dynamic adsorptive removal of selenite and selenate by alkoxide-free sol–gel-generated Mg–Al–CO_3 layered double hydroxide: effect of competing ions, Chem. Eng. J. 279 (2015) 885–896.
[21] S.V. Prasanna, P.V. Kamath, Chromate uptake characteristics of the pristine layered double hydroxides of Mg with Al, Solid State Sci. 10 (2008) 260–266.
[22] D. Wan, H. Liu, R. Liu, J. Qu, S. Li, J. Zhang, Adsorption of nitrate and nitrite from aqueous solution onto calcined (Mg–Al) hydrotalcite of different Mg/Al ratio, Chem. Eng. J. 195–196 (2012) 241–247.
[23] M. Everaert, R. Warrinnier, S. Baken, J.P. Gustafsson, D. De Vos, E. Smolders, Phosphate-Exchanged Mg–Al layered double hydroxides: a new slow release phosphate fertilizer, ACS Sustainable Chem. Eng. 4 (2016) 4280–4287.
[24] D.L. Sparks, Kinetics of Soil Chemical Processes, Academic Press, London, 1989.
[25] M. Jobbágy, A.E. Regazzoni, Dissolution of nano-size Mg–Al–Cl hydrotalcite in aqueous media, Appl. Clay Sci. 51 (2011) 366–369.
[26] Y.S.R. Chen, J.N. Butler, W. Stumm, Kinetic study of phosphate reaction with aluminum oxide and kaolinite, Environ. Sci. Technol. 7 (1973) 327–332.
[27] C. Luengo, M. Brigante, M. Avena, Adsorption kinetics of phosphate and arsenate on goethite. A comparative study, J. Colloid Interface Sci. 311 (2007) 354–360.
[28] J. Murphy, J.P. Riley, A modified single solution method for the determination of phosphate in natural waters, Anal. Chim. Acta 27 (1962) 31–36.
[29] Y. Gao, A. Mucci, Acid base reactions phosphate and arsenate complexation, and their competitive adsorption at the surface of goethite in 0.7 M NaCl solution, Geochim. Cosmochim. Acta 65 (2001) 2361–2378.
[30] R.J. Hunter, Zeta Potential in Colloid Science: Principles and Applications, Academic Press, London, 1981.
[31] R. Rojas, M.A. Ulibarri, C. Barriga, V. Rives, Intercalation of metal-edta complexes in Ni–Zn layered hydroxysalts and study of their thermal stability, Micropor. Mesopor. Mat. 112 (2008) 262–272.
[32] M. Zhang, B. Gao, Y. Yao, M. Inyang, Phosphate removal ability of biochar/MgAl-LDH ultra-fine composites prepared by liquid-phase deposition, Chemosphere 92 (2013) 1042–1047.
[33] M. Yoshida, P. Koilraj, X. Qiu, T. Hirajima, K. Sasaki, Sorption of arsenate on MgAl and MgFe layered double hydroxides derived from calcined dolomite, J. Environ. Chem. Eng. 3 (2015) 1614–1621.
[34] K.S. Triantafyllidis, E.N. Peleka, V.G. Komvokis, P.P. Mavros, Iron-modified hydrotalcite-like materials as highly efficient phosphate sorbents, J. Colloid Interf. Sci. 342 (2010) 427–436.
[35] S. Miyata, The syntheses of hydrotalcite-like compounds and their structures and physico-chemical properties I: the systems Mg^{2+}-Al^{3+}-NO_3^-, Mg^{2+}-Al^{3+}-Cl^-, Mg^{2+}-Al^{3+}-ClO_4^-, Ni^{2+}-Al^{3+}-Cl^- and Zn^{2+}-Al^{3+}-Cl^-, Clay. Clay Miner. 23 (1975) 369–375.
[36] R.L. Frost, A.W. Musumeci, M. Adebajo, W. Martens, Using thermally activated hydrotalcite for the uptake of phosphate from aqueous media, J. Therm. Anal. Calorim. 89 (2007) 95–99.
[37] A. Ookubo, K. Ooi, H. Hayashi, Preparation and phosphate ion-exchange properties of a hydrotalcite-like compound, Langmuir 9 (1993) 1418–1422.
[38] K.H. Goh, T.T. Lim, A. Banas, Z. Dong, Sorption characteristics and mechanisms of oxyanions and oxyhalides having different molecular properties on Mg/Al layered double hydroxide nanoparticles, J. Hazard. Mater. 179 (2010) 818–827.
[39] J. Zhou, S. Yang, J. Yu, Z. Shu, Novel hollow microspheres of hierarchical zinc–aluminum layered double hydroxides and their enhanced adsorption capacity for phosphate in water, J. Hazard. Mater. 192 (2011) 1114–1121.
[40] Q. Yu, Y. Zheng, Y. Wang, L. Shen, H. Wang, Y. Zheng, N. He, Q. Li, Highly selective adsorption of phosphate by pyromellitic acid intercalated ZnAl-LDHs: assembling hydrogen bond acceptor sites, Chem. Eng. J. 260 (2015) 809–817.
[41] T. Kameda, E. Kondo, T. Yoshioka, Equilibrium and kinetics studies on As(V) and Sb (V) removal by Fe2+-doped Mg-Al layered double hydroxides, J. Environ. Management 151 (2015) 303–309.
[42] Y. Seida, Y. Nakano, Removal of phosphate by layered double hydroxides containing iron, Water Res. 36 (2002) 1306–1312.
[43] S.H. Han, W.G. Hou, C.G. Zhang, D.J. Sun, X.R. Huang, G.T. Wang, Structure and the point of zero charge of magnesium aluminum hydroxide, J. Chem. Soc. Faraday Trans. 9 (1998) 915–918.
[44] K. Morimoto, S. Anraku, J. Hoshino, T. Yoneda, T. Sato, Surface complexation reactions of inorganic anions on hydrotalcite-like compounds, J. Colloid Interf. Sci. 384 (2012) 99–104.
[45] G. Akay, B. Keskinler, A. Cakici, U. Danis, Phosphate removal from water by red mud using crossflow microfiltration, Water Res. 32 (1998) 717–726.
[46] A. Ugurlu, B. Salman, Phosphate removal from water by fly ash, Environ. Int. 24 (1998) 911–918.
[47] M. Ozacar, Equilibrium and kinetic modeling of adsorption of phosphorus on calcined alunite, Adsorption 9 (2003) 125–132.
[48] H. Brattebo, H. Odegaard, Phosphorus removal by granular activated alumina, Water Res. 20 (1986) 977–986.
[49] C. Namasivayam, D. Sangeetha, Equilibrium and kinetic studies of adsorption of phosphate onto ZnCl2 activated coir pith carbon, J. Colloid Interf. Sci. 280 (2004) 359–365.
[50] K.M. Parida, S. Mallick, S.S. Dash, Studies on manganese nodule leached residues 2. Adsorption of aqueous phosphate on manganese nodule leached residue, J. Colloid Interf. Sci. 290 (2005) 22–27.
[51] C. Luengo, M. Brigante, J. Antelo, M. Avena, Kinetics of phosphate adsorption on goethite: comparing batch adsorption and ATR-IR measurements, J. Colloid Interf. Sci. 300 (2006) 511–518.
[52] X.-H. Wang, F.-F. Liu, L. Lu, S. Yang, Y. Zhao, L.-B. Sun, S.-G. Wang, Individual and competitive adsorption of Cr (VI) and phosphate onto synthetic Fe–Al hydroxides, Colloids Surf. A 423 (2013) 42–49.
[53] S. Tanada, M. Kabayama, N. Kawasaki, T. Sakiyama, T. Nakamura, M. Araki, T. Tamura, Removal of phosphate by aluminum oxide hydroxide, J. Colloid Interf. Sci. 257 (2003) 135–140.
[54] R. Chitrakar, S. Tezuka, A. Sonoda, K. Sakane, K. Ooi, T. Hirotsu, Phosphate adsorption on synthetic goethite and akaganeite, J. Colloid Interf. Sci. 298 (2006) 602–608.
[55] G. Zhang, H. Liu, R. Liu, J. Qu, Removal of phosphate from water by a Fe-Mn binary oxide adsorbent, J. Colloid Interf. Sci. 335 (2009) 168–174.
[56] H. Liu, X. Sun, C. Yin, C. Hu, Removal of phosphate by mesoporous ZrO_2, J. Hazard. Mater. 151 (2008) 616–622.
[57] R. Saad, K. Belkacemi, S. Hamoudi, Adsorption of phosphate and nitrate anions on ammonium-functionalized MCM-48: effects of experimental conditions, J. Colloid Interf. Sci. 311 (2007) 375–381.
[58] J. Lu, H. Liu, R. Liu, X. Zhao, L. Sun, J. Qu, Adsorptive removal of phosphate by a nanostructured Fe–Al–Mn trimetal oxide adsorbent, Powder Technol. 233 (2013) 146–154.
[59] S. Ouvrard, M.-O. Simonnot, M. Sardin, Reactive behaviour of natural manganese oxides towards the adsorption of phosphate and arsenate, Ind. Eng. Chem. Res. 41 (2002) 2785–2791.
[60] P. Ning, H.-J. Bart, B. Li, X. Lu, Y. Zhang, Phosphate removal from wastewater by model-La(III) zeolite adsorbents, J. Environ. Sci. 20 (2008) 670–674.
[61] S. Tezuka, R. Chitrakar, K. Sakane, A. Sonoda, K. Ooi, T. Tomida, The synthesis and phosphate adsorptive properties of Mg(II)–Mn(III) LDH and their heat-treated materials, Bull. Chem. Soc. Jpn. 77 (2004) 2101–2107.
[62] H.S. Shin, M.J. Kim, S.Y. Nam, H.C. Moon, Phosphorus removal by hydrotalcite-like compounds (HTLcs), Water Sci. Technol 34 (1996) 161–168.
[63] M. Khitous, Z. Salem, D. Halliche, Removal of phosphate from industrial wastewater using uncalcined MgAl-NO_3 layered double hydroxide: batch study and modeling, Desalin. Water Treat. 57 (2016) 15920–15931.
[64] A. Bakhti, M.S. Ouali, Sorption of phosphate ions on a calcined synthetic hydrotalcite, Ann. Chim. Sci. Mater. 31 (2006) 407–420.